

Single Turnover Active Fluorometry (STAF) - additional material...

Kevin Oxborough^{1,2}, Nina Schuback^{1,3}, Mary Burkitt-Gray¹, Alan Wright² and Mark Moore²

¹Chelsea Technologies Ltd., West Molesey, KT8 2QZ, UK

²University of Southampton at NOCS, Southampton, SO14 3ZH, UK

³Swiss Polar, Institute, Rue de l'Industrie 17, 1950 Sion, Switzerland



The Photochemical Excitation profile (PEP)²

As noted within Poster 1, the main application for PEP data is to facilitate spectral correction of J_{PII} and JV_{PII} . RunSTAF calculates waveband-specific values of F_v and σ_{PII} . While the F_v PEP values are largely unaffected by spectral heterogeneity within the sample, the σ_{PII} PEP values are not. For this reason, only the F_v PEP values are used to correct J_{PII} and JV_{PII} .

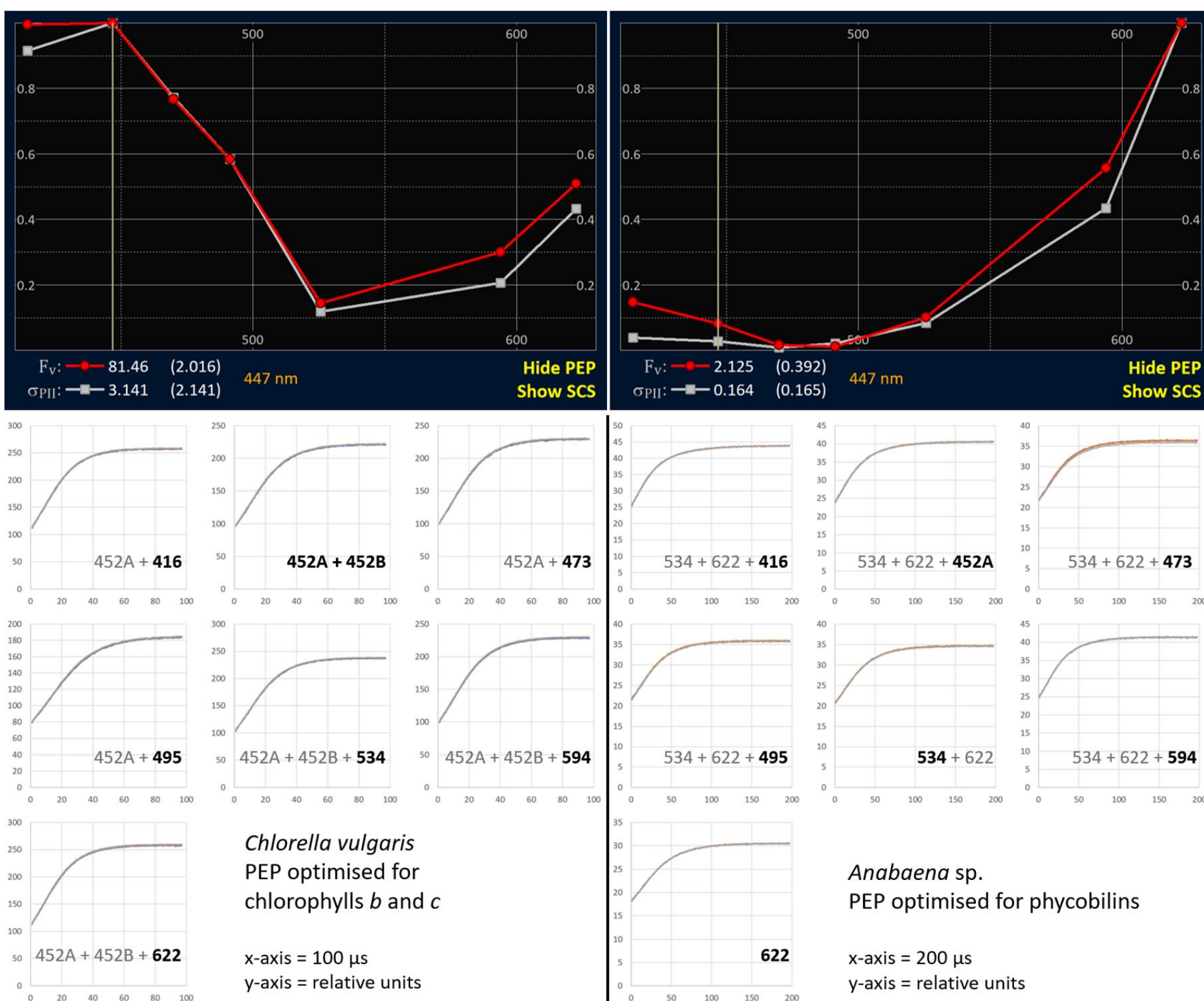


Figure 1: The PEP is constructed by averaging a user-set number of ST curves for each combination of wavebands. The LabSTAF or AutoSTAF unit cycles through the list of Steps until the required number of curves have been acquired. Using optimal combinations of LEDs ensures that a high enough proportion of functional PSII complexes are closed during the ST pulse to generate accurate values of F_v and σ_{PII} .

Figure 2: provides some examples of F_v and σ_{PII} PEPs. Examples E and J show the largest differences between the two PEPs and are likely to include cyanobacterial contamination.

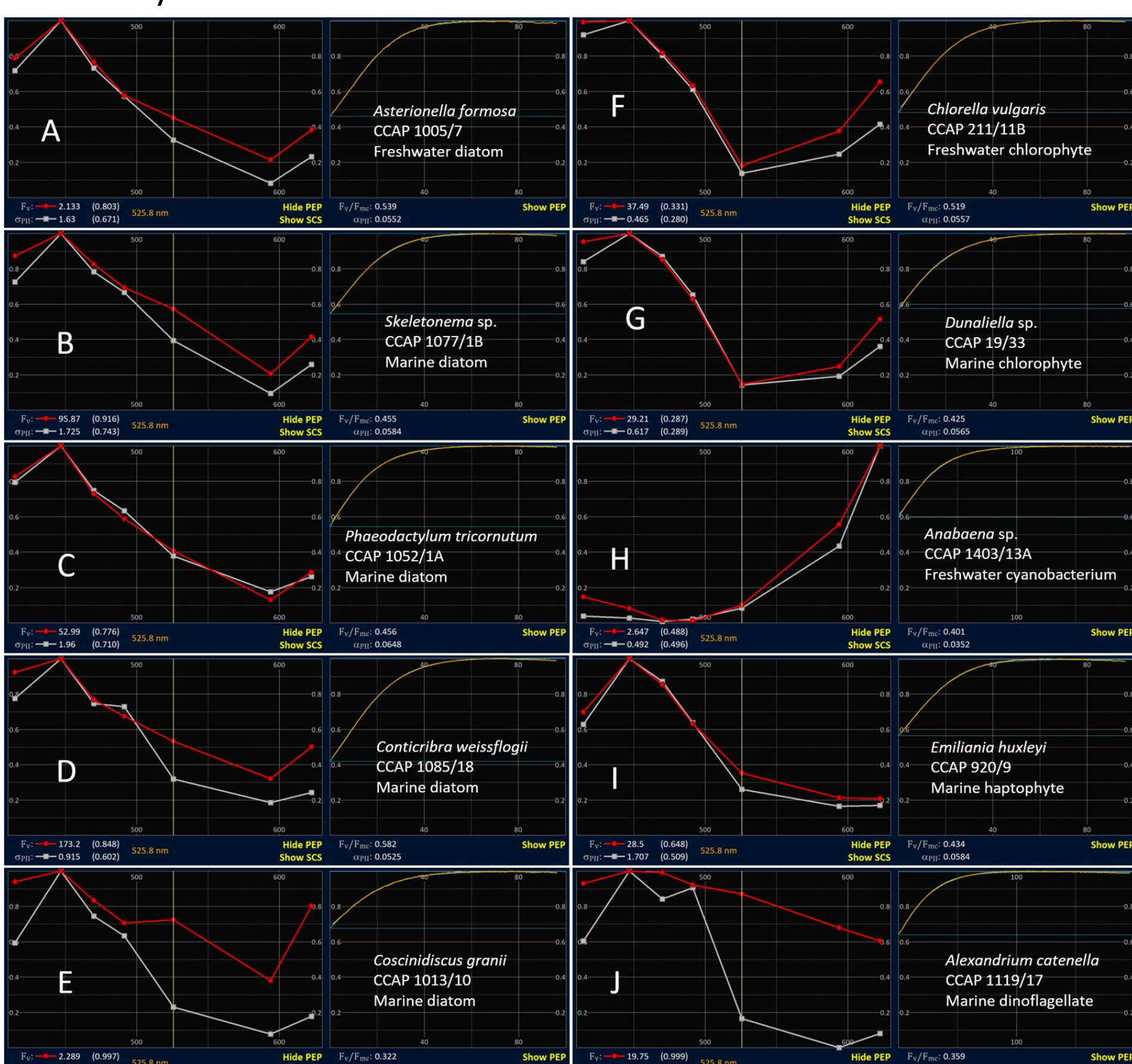


Figure 2: Representative PEP plus ST pulse for each of ten phytoplankton species.

Baseline fluorescence^{1,2}

The fraction of F_0 that does not originate from photochemically active PSII complexes is termed baseline fluorescence and is quantified as F_b . Baseline fluorescence introduces an error into the calculation of a number of fluorescence parameters, including JV_{PII} . The data plots within **Figure 3** illustrate the impact of baseline correction on the match between STAF-derived assessment of PSII photochemistry and gross oxygen release measured with a Clark-type electrode.

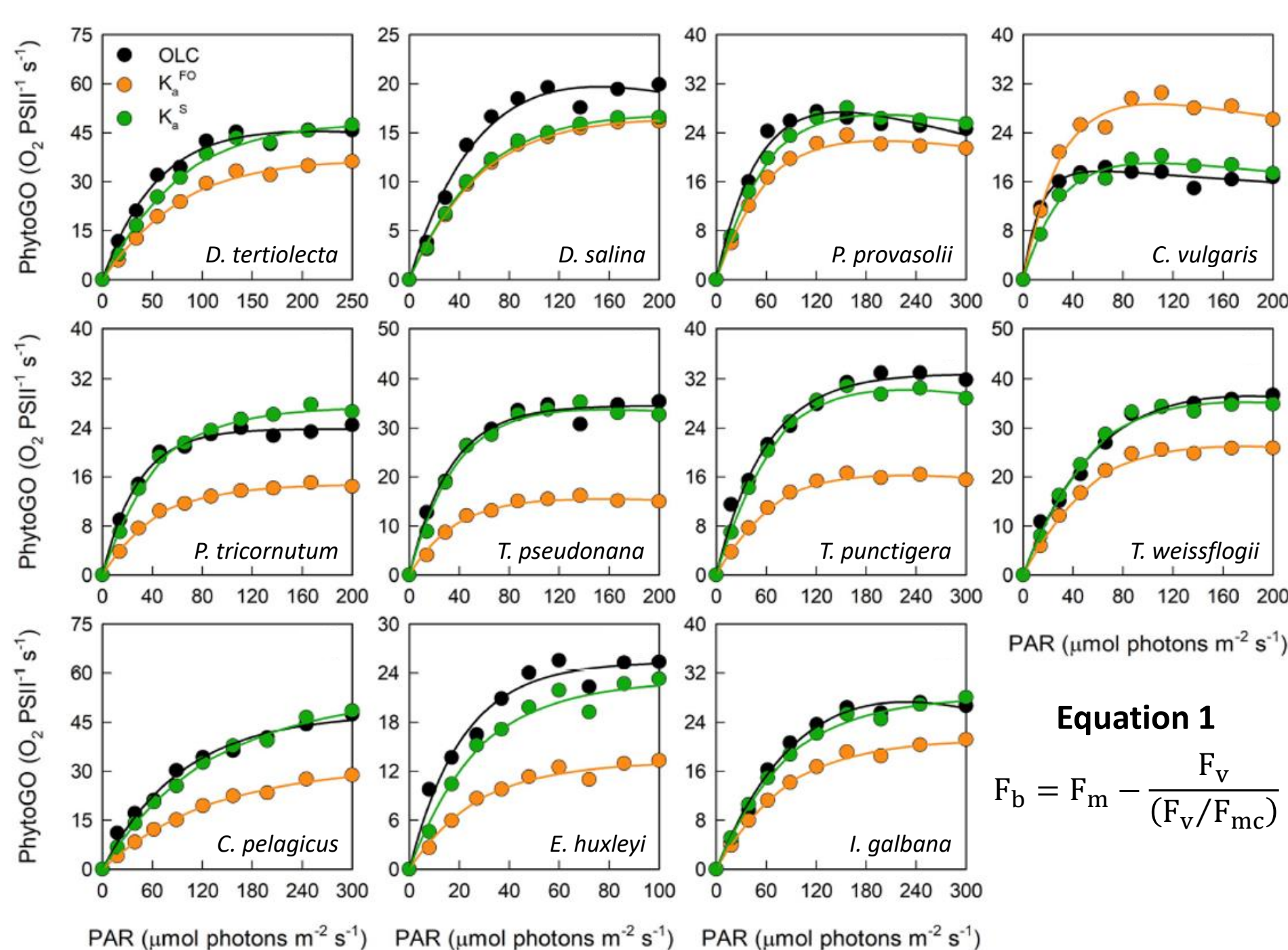


Figure 3: Simultaneous Oxygen Light Curve (OLC) and Fluorescence Light Curve (FLC) measurements made across a range of phytoplankton species. Measurements were made on cultures acclimated to $\sim 20^\circ\text{C}$ and $30 \mu\text{mol photons m}^{-2} \text{s}^{-1}$. FLC data were standardized to equivalent units of O_2 , with both OLC and FLC data normalized to a derived concentration of functional PSII complexes ($\text{O}_2 \text{ PSII}^{-1} \text{ s}^{-1}$). FLC data were derived using K_s^{F0} ($11,800 \text{ m}^{-1}$) or a sample-specific (K_s^S) value. The solid lines represent the P-E curve fits. The K_s^S values were generated by applying an intrinsic F_v/F_m ($F_v/F_{m,c}$) of 0.518 across all species (**Equation 1**). These data were originally presented by Boatman et al. 2019.

The dual ST pulse measurement²

The Dual ST Pulse (DSP) method incorporated within the STAF systems described here tracks the reopening of PSII complexes that are closed by the first ST pulse in the sequence. The paired ST pulses are normally of the same duration, with a variable gap between them (**Figure 4**).

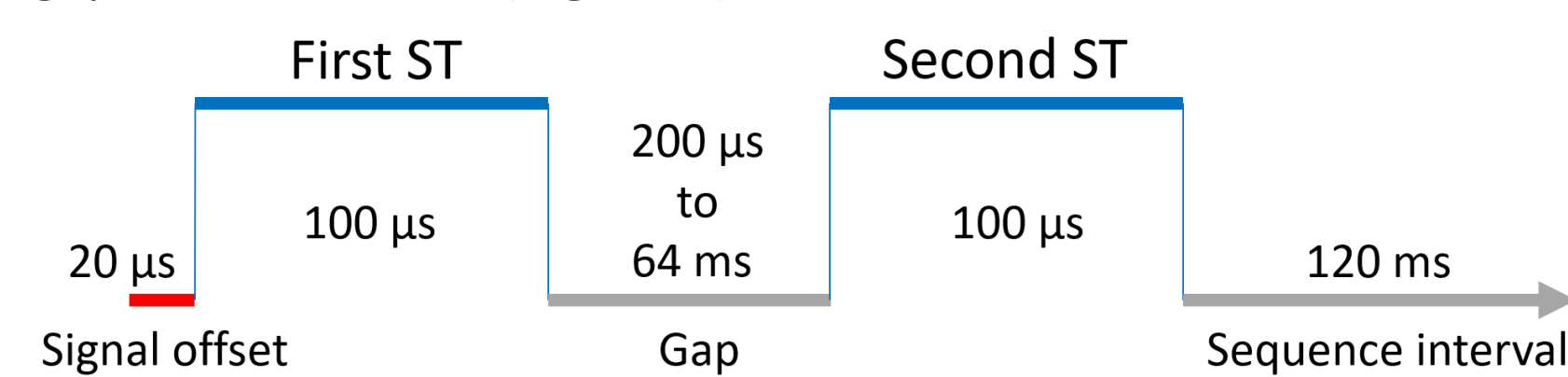


Figure 4: The DSP sequence starts 20 μs before the first ST pulse is applied. Data are logged at 1 MHz during this Signal offset and during the First ST and Second ST pulses. No data are logged during the Gap or Sequence interval.

The default set incorporates 11 DSPs, with gaps of between 400 μs and 12800 μs between the end of the first ST pulse and the start of the second ST pulse. RunSTAF sets the gap sequences such that the increase in gap duration between successive pairs is constant through the entire set. This arithmetic progression is clear within the example below, which incorporate 6 DSPs with gaps of between 200 μs and 6400 μs .

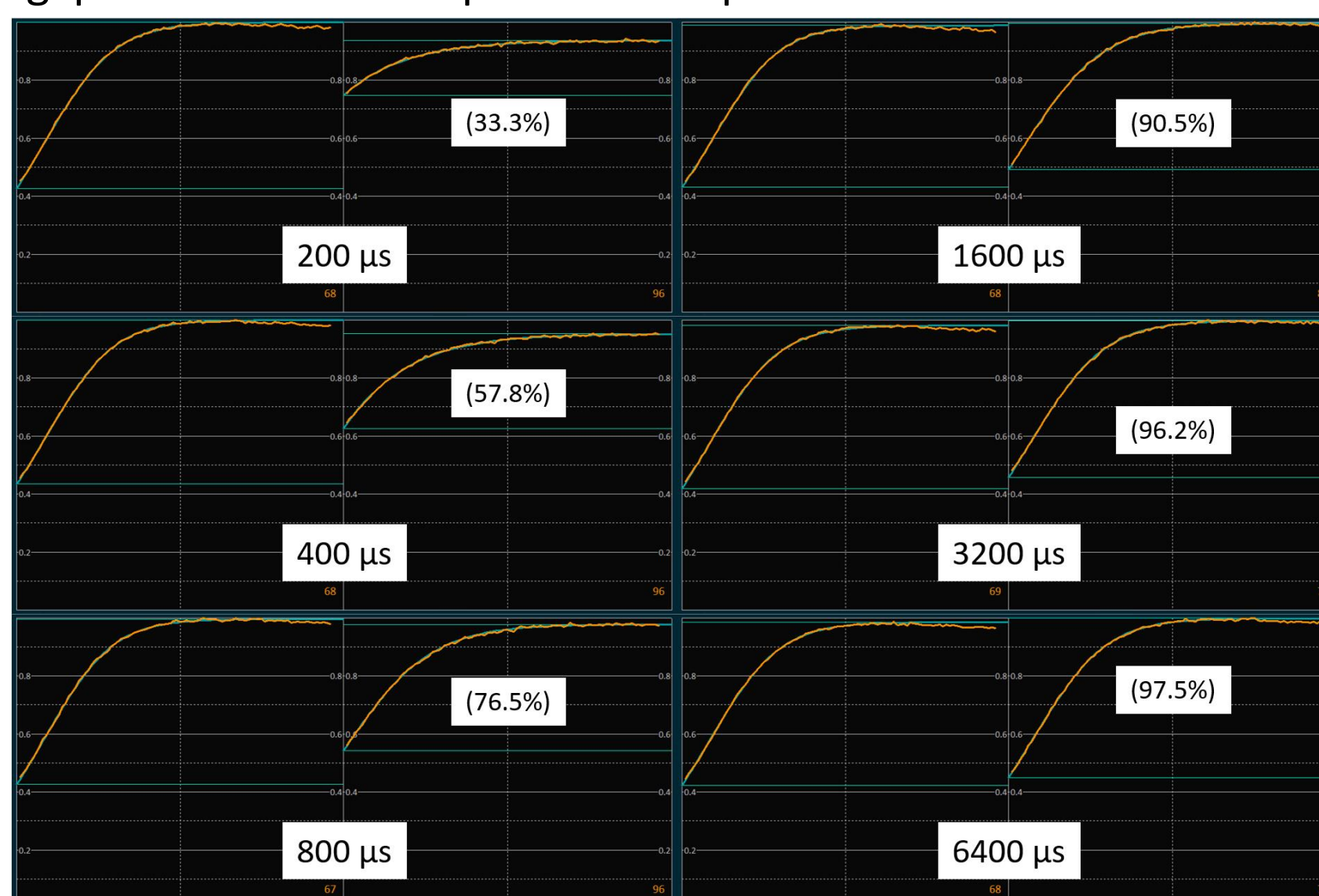


Figure 5: Composite from RunSTAF screenshots showing six DSP pairs within a set. The target sample was dark adapted. The times shown are the gap intervals. The numbers within brackets are % recovery of variable fluorescence between the first and second ST pulse.

RunSTAF generates three fits to the DSP dataset, as shown in **Figure 6**. The first is based on a simple recovery of F_v (**Fv**) as shown in **Figure 5**. The second and third fits track the reopening of centres based on homogeneous connectivity (**Rho**) and dimerization of PSII complexes (**Dimer**). The three fits show the largest divergence in the dark and decreasing divergence with increasing actinic E. All three fits incorporate a fast and a slow phase. It is assumed that the fast phase is dominated by the reopening of PSII with plastoquinone or semi-plastoquinone bound at the Q_b site at the end of the first ST pulse while the slow phase is dominated by the reopening of RCII with an empty Q_b site at the end of the first ST pulse. Δ_F and Δ_S are the proportions of the total amplitude of the relaxation phase attributable to the fast and slow phases, respectively. τ_F and τ_S are the time constants for the fast and slow phases, respectively.

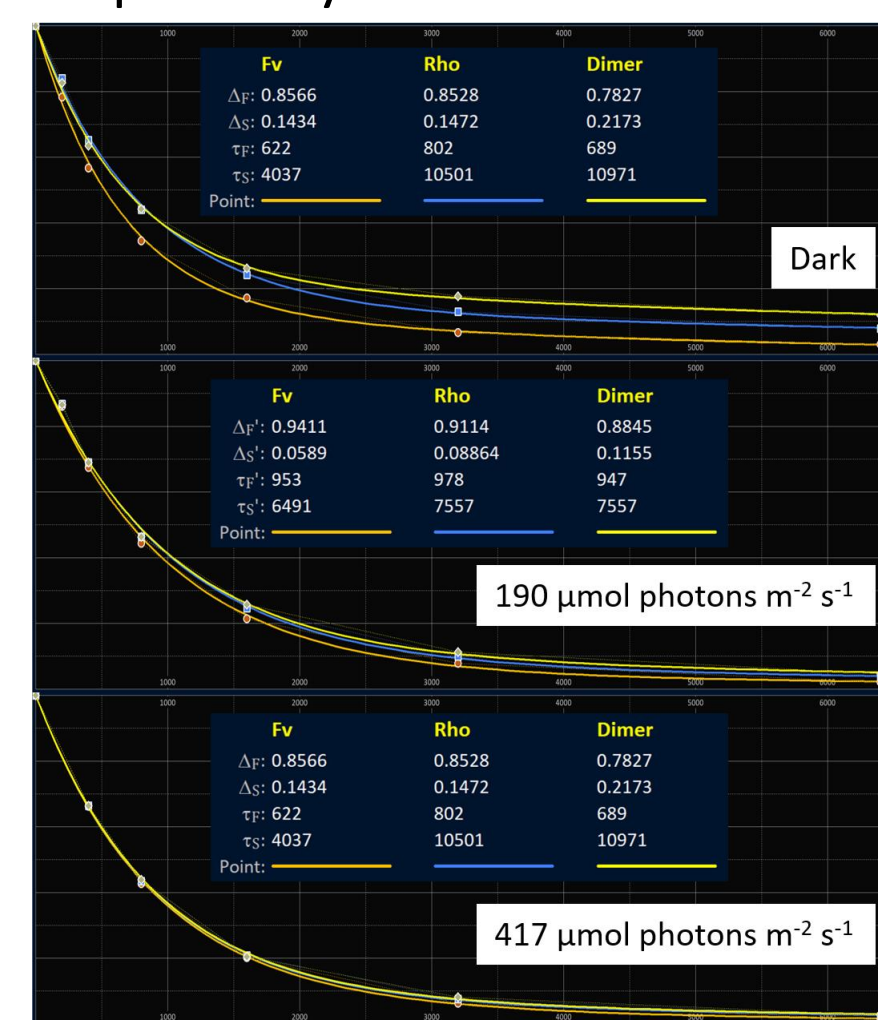


Figure 6: Composite screenshots showing relaxation phase fits from complete DSP datasets from a sample in the dark and at two actinic light levels. **Equation 2** provides the basic structure for all three curve fits (**Fv**, **Rho** and **Dimer**). For the **Rho** and **Dimer** fits, the F values are replaced with the proportion of PSII complexes in the open state.

$$\text{Equation 2} \\ F_t = F_v \cdot \left(\Delta_F \cdot e^{-\frac{t}{\tau_F}} + \Delta_S \cdot e^{-\frac{t}{\tau_S}} \right)$$

A PSII dimer model for ST fits²

The dimer fits to ST data within RunSTAF incorporate the following simple assumptions:

- The two PSII reaction centres within each dimer are perfectly connected (share the same light-harvesting system)
- There is no connectivity among dimers

Although these assumptions impose significant restrictions on the ST curve fitting process, the 'goodness of fit' is generally very close to the less restrictive Rho fit, which allows the connectivity among PSII complexes to float.

The example DSP in **Figure 7** includes the dimer fit. The [oo], [oc] and [cc] are: both PSII reaction centres open, one open and one closed and both closed, respectively.

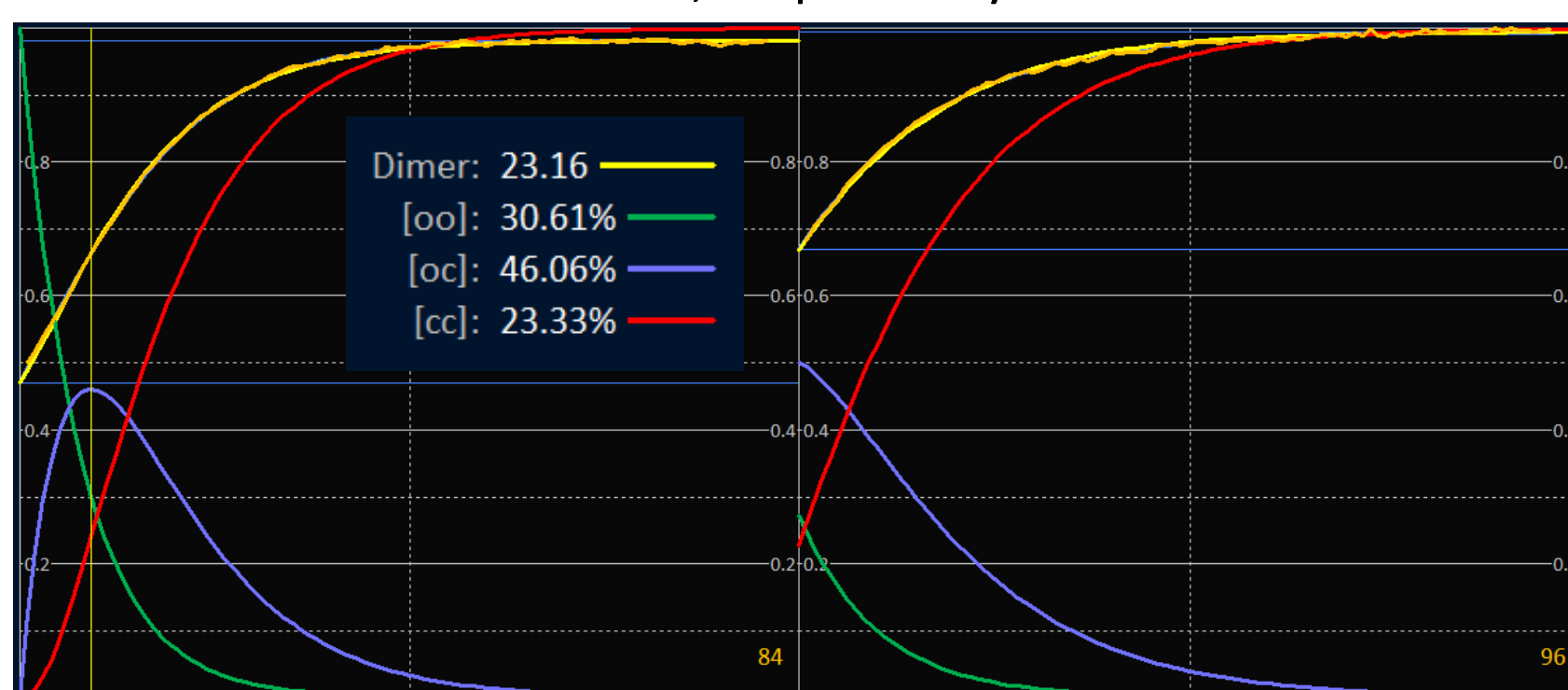


Figure 7: A DSP from a dark-adapted sample illustrating the dimer fit. The gap between the end of the first ST pulse and the start of the second ST pulse was 800 μs . The proportions of [oo], [oc] and [cc] shown in the legend are at the point selected within the first ST pulse (the vertical yellow line). The starting points for the [oo], [oc] and [cc] lines on the second ST pulses assume an equal probability of a closed PSII reaction centre reopening within an [oc] or [cc] during the gap between the two ST pulses.

ST pulse-induced quenching of σ_{PII} ²

One consistent and surprising observation from application of the DSP method is a rapid, transient decrease in σ_{PII} , such that the second ST pulse value ($\sigma_{PII}^{(2)}$) is as much as 50% lower than the first ST pulse value (**Figure 8**). The 'recovery' time for this decrease is low hundreds of μs and the kinetics of this recovery (**Figure 9**) are consistent with connectivity among PSII complexes being limited to dimerization.

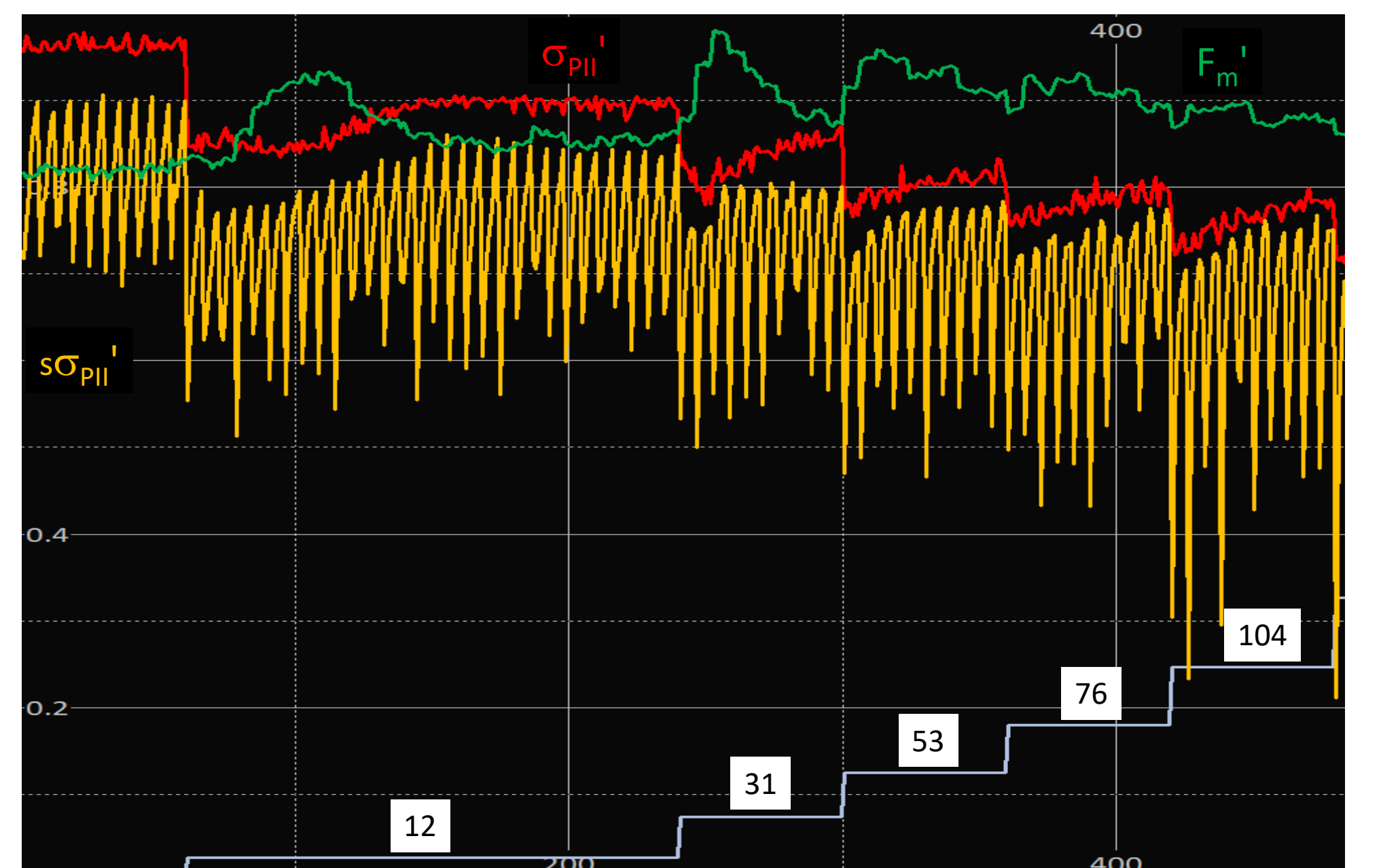


Figure 8: Crop from the RunSTAF data screen showing changes in $\sigma_{PII}^{(1)}$, $\sigma_{PII}^{(2)}$ and $F_m^{(2)}$ during the first steps of an FLC. The numbers in white squares are incident E ($\mu\text{mol photons m}^{-2} \text{s}^{-1}$). The oscillations in $\sigma_{PII}^{(1)}$ track the gap steps during each DSP.

On the assumption that charge separation at a closed PSII is best avoided, dimerization of PSII can be seen as being photoprotective. The protection is provided to a closed PSII within an open plus closed (oc) dimer, simply because an absorbed photon is more likely to result in charge separation at the open PSII than the closed PSII.

The observed decrease in σ_{PII} after an ST pulse may also reflect a photoprotective process, that could operate within double closed (cc) dimers. The working assumption is that the apparent 50% decrease in σ_{PII} observed within the DSP measurements reflects a requirement for two photochemical events to close an open PSII in the first few hundred μs after formation of the cc dimer. In turn, it is assumed that this requirement is indicative of a deexcitation pathway within a closed PSII that is functional over that timescale. Although this pathway could only operate once, within the relevant timescale, the protection provided (against what is already an infrequent event in most situations) could be highly effective.

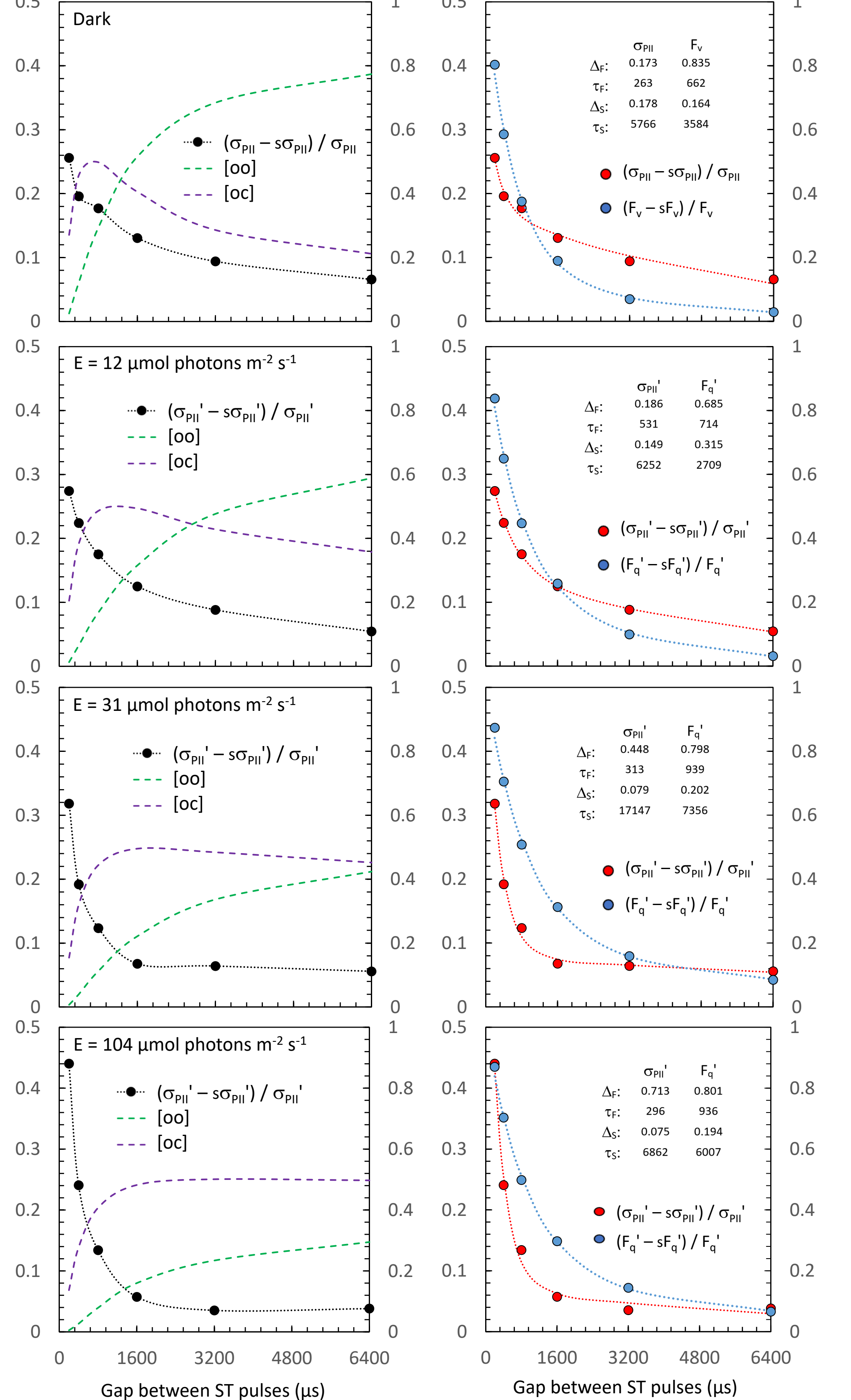


Figure 9: The left column shows the recovery of $\sigma_{PII}^{(1)}$ with concurrent changes in [oo] and [oc]. The right column shows concurrent changes the recovery of $\sigma_{PII}^{(2)}$ and F_v or $F_m^{(2)}$. The increase in [oc] relative to [oo] and the amplitude of the fast phase (Δ_F) of the $\sigma_{PII}^{(1)}$ recovery, within increasing E, are consistent with PSII dimerization being the main basis for connectivity among PSII complexes.

References:

- Boatman, T.G., Geider R.J. and Oxborough, K. (2019) Improving the accuracy of single turnover active fluorometry (STAF) for the estimation of phytoplankton primary productivity (PhytoPP). *Front. Mar. Sci.* <https://doi.org/10.3389/fmars.2019.00319>
- Oxborough, K., Schuback, N., Burkitt-Gray, M., Moore, C.M. and others (2022) LabSTAF and RunSTAF handbook. Chelsea Technologies Ltd.